UNCLASSIFIED
SECURITY CLASSIFICATION OF THIS PAGE

AFIT FILE COPY (2)

REPORT DOCUMENTATION PAGE

Form Approved
OMB No. 0704-0188

1a. REPORT SECURITY CLASSIFICATION
UNCLASSIFIED

1b. RESTRICTIVE MARKINGS

DTIC

AD-A213 395

ELECTE
OCT 05 1989
D

3. DISTRIBUTION/AVAILABILITY OF REPORT
Approved for public release, distribution is unlimited.

5. MONITORING ORGANIZATION REPORT NUMBER(S)
AFATL-TP-89-18

6a. NAME OF PERFORMING ORGANIZATION	6b. OFFICE SYMBOL (If applicable)	7a. NAME OF MONITORING ORGANIZATION
Aerodynamics Branch Aeromechanics Division	AFATL/FXA	Aerodynamics Branch Aeromechanics Division

6c. ADDRESS (City, State, and ZIP Code)	7b. ADDRESS (City, State, and ZIP Code)
Air Force Armament Laboratory Eglin Air Force Base, Florida 32542-5434	Air Force Armament Laboratory Eglin Air Force Base, Florida 32542-5434

8a. NAME OF FUNDING/SPONSORING ORGANIZATION	8b. OFFICE SYMBOL (If applicable)	9. PROCUREMENT INSTRUMENT IDENTIFICATION NUMBER
Air Force Office of Scientific Research	AFOSR/NA	

8c. ADDRESS (City, State, and ZIP Code)	10. SOURCE OF FUNDING NUMBERS			
	PROGRAM ELEMENT NO.	PROJECT NO.	TASK NO	WORK UNIT ACCESSION NO.
Bolling Air Force Base, D.C.	61102F	2307	E1	30

11. TITLE (Include Security Classification)

Transonic Euler Solutions on Mutually Interfering Finned Bodies

12. PERSONAL AUTHOR(S)
Lawrence E. Lijewski

13a. TYPE OF REPORT	13b. TIME COVERED	14. DATE OF REPORT (Year, Month, Day)	15. PAGE COUNT
Final	FROM Oct 83 TO Sep 89	Sep 89	10

16. SUPPLEMENTARY NOTATION

17. COSATI CODES			18. SUBJECT TERMS (Continue on reverse if necessary and identify by block number)
FIELD	GROUP	SUB-GROUP	
01	01		Numerical Grid Generation; Finned Bodies; Euler Equations; Transonic Flows; Mutual Interference; Forces and Moments

19. ABSTRACT (Continue on reverse if necessary and identify by block number)

The ability of an Euler code to predict mutual aerodynamic interference in the transonic regime was investigated. One, two, and three body combinations of a cruciform finned configuration were examined at Mach numbers from 0.80 to 1.20 and angles of attack up to ten degrees. Predicted surface pressure distributions were compared with wind tunnel data for the first time on three finned bodies with success. The Euler code was found to predict body pressures well in many interference regions, although shock location often was less accurate due to viscous effects in the strongest interference flowfield near Mach 1. Rigid body physics of the three body combination was investigated from integrated pressure distributions. Force and moment behavior was found to be strongly dependent upon Mach number.

20. DISTRIBUTION/AVAILABILITY OF ABSTRACT	21. ABSTRACT SECURITY CLASSIFICATION
☐ UNCLASSIFIED/UNLIMITED ☒ SAME AS RPT ☐ DTIC USERS	UNCLASSIFIED

22a. NAME OF RESPONSIBLE INDIVIDUAL	22b. TELEPHONE (Include Area Code)	22c. OFFICE SYMBOL
Lawrence E. Lijewski	904-882-3124	AFATL/FXA

DD Form 1473, JUN 86 — Previous editions are obsolete. — SECURITY CLASSIFICATION OF THIS PAGE UNCLASSIFIED

AIAA '89

AIAA-89-0264
Transonic Euler Solutions on Mutually Interfering Finned Bodies

Lawrence E. Lijewski
U.S. Air Force Armament Laboratory
Eglin Air Force Base, Florida

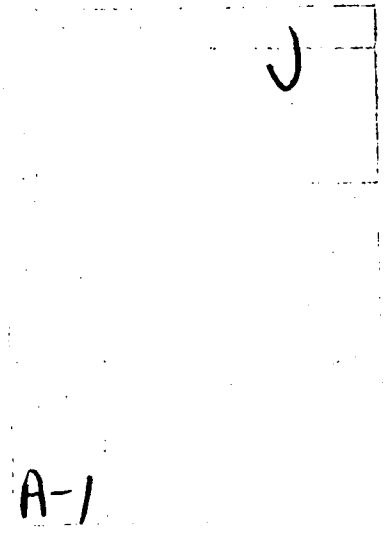

A-1

27th Aerospace Sciences Meeting
January 9-12, 1989/Reno, Nevada

TRANSONIC EULER SOLUTIONS

ON MUTUALLY INTERFERING FINNED BODIES

*Lawrence E. Lijewski**
Aerodynamics Branch
Aeromechanics Division
Air Force Armament Laboratory
Eglin Air Force Base, Florida 32542

Abstract

The ability of an Euler code to predict mutual aerodynamic interference in the transonic regime was investigated. One, two, and three body combinations of a cruciform finned configuration were examined at Mach numbers from 0.80 to 1.20 and angles of attack up to ten degrees. Predicted surface pressure distributions were compared with wind tunnel data for the first time on three finned bodies with success. The Euler code was found to predict body pressures well in many interference regions, although shock location often was less accurate due to viscous effects in the strongest interference flowfield near Mach 1. Rigid body physics of the three body combination was investigated from integrated pressure distributions. Force and moment behavior was found to be strongly dependent upon Mach number.

Nomenclature

Cp	Pressure coefficient
Cp*	Sonic pressure coefficient
Cmy	Yawing moment coefficient
Cmz	Pitching moment coefficient
Cy	Yaw force coefficient
Cz	Normal force coefficient
FS	Freestream condition
L	Lower body
U	Upper body
X/C	Axial location per local chord length
X/L	Axial location per body length
ϕ	Angular position

Introduction

It is widely recognized that speed, range, and endurance of fighter aircraft is influenced by the aerodynamic forces generated by mutually interfering bodies in external carriage. In addition, the release of these bodies from the parent aircraft is highly dependent on their aerodynamic interrelationship when in close proximity. This influence is most pronounced in the transonic regime where modern tactical fighters often operate. Until recently, it has been difficult to numerically predict the aerodynamic flowfield about mutually interfering bodies in the transonic Mach range, where embedded regions of subsonic and supersonic flow preclude the use of marching codes. With the advent of generalized, arbitrary geometry, multi-block grid codes[1, 2] and sophisticated flow solvers[3, 4] to work in concert with these grids, good engineering solutions can be obtained on complex configurations.[5, 6] Flow calculations have been successfully obtained on multiple unfinned bodies[7, 8] and two finned bodies[9] at low angles of attack. Realistic flight conditions dictate the necessity of predicting interference aerodynamics for multiple finned bodies at low to moderate angles of attack.

The purpose of this paper is twofold; first, to investigate the ability of an Euler code to predict mutual aerodynamic interference, and second, to examine the characteristic physics that occurs in the transonic regime when finned bodies are placed in close proximity. Interference effects will be explored by comparing pressure distributions for one, two, and three finned bodies with wind tunnel data. Force and moment calculations for the three finned body case will be examined along with oil flows and pressure distributions to attempt to explain the mutual aerodynamic phenomena occurring between Machs 0.80 and 1.20.

Configurations

The basic body geometry, Figure 1, consists of a tangent ogive forebody, cylindrical centerbody, and tangent ogive afterbody, truncated to mount on a sting. Each of the cruciform fins has a NACA 0008 airfoil cross section with exposed aspect ratio of 0.257. The finned body was arranged in single, double, and triple combinations as illustrated in Figure 2. The separation distance between body centerlines was 1.5 body diameters for both the double and triple configurations. Surface pressure data was obtained at 198 pressure taps, which were situated in four longitudinal rows on the body, and eight spanwise rows on the fins. The positive angular orientation is as shown with zero always at the top of each body.

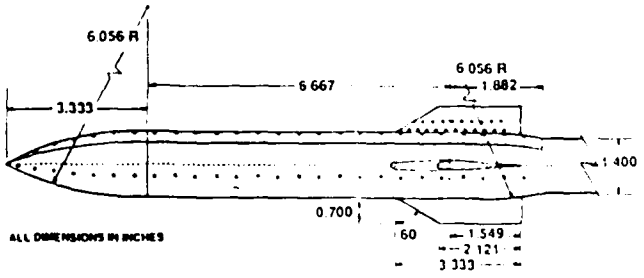

Fig. 1 Finned Body Geometry

* Research Scientist
Senior Member, AIAA

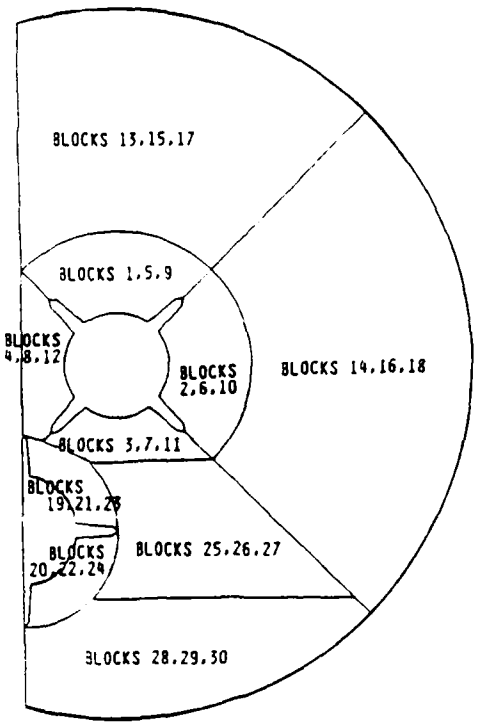

Fig. 5 Blocking Scheme, 3-Body Case

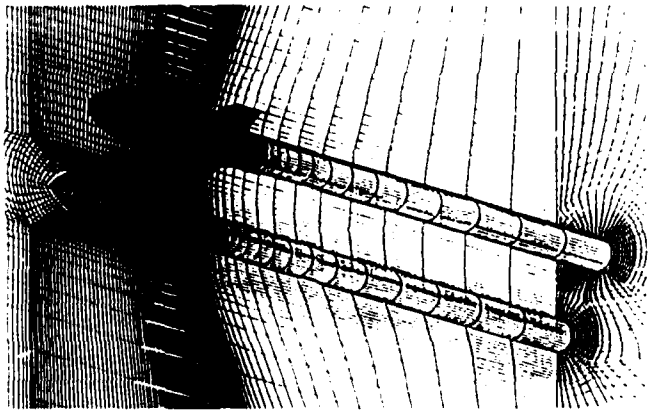

Fig. 6 Reflection and Back Planes, 3-Body Case

seven blocks each stacked axially. The dimensions of blocks 1-12 are identical to those in the three body case, with the same grid spacings maintained whenever possible. The wireframe grid cross-section for the single body configuration is shown in Figure 8. This grid is now 24 blocks (289,432 points), simply by adding three outer boundary blocks where the reflection plane was located in Figure 7. Here the size of the first 21 blocks are the same as before with the same spacing enforced where possible.

Computational Results

The flow solver used was the Euler code developed by Belk, Whitfield, et al[4]. The solver is an implicit, two-pass, upwind scheme, second order accurate in space. It solves the flux-

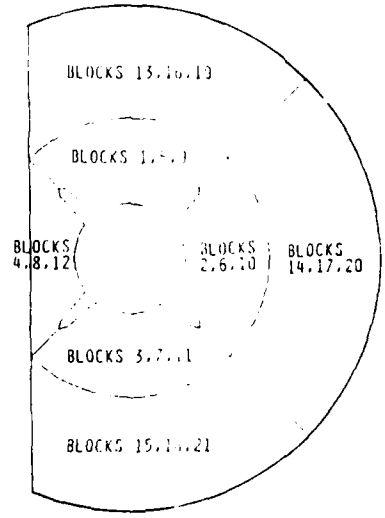

Fig. 7 Blocking Scheme, 2-Body Case

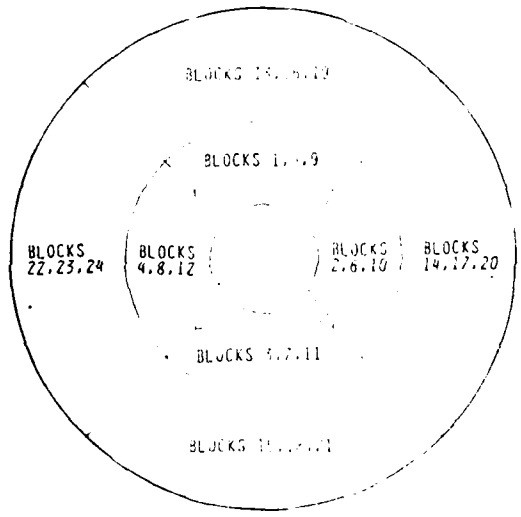

Fig. 8 Blocking Scheme, 1-Body Case

difference-split form of the Euler equations using a modified Roe scheme that is stable for a wide range of Courant numbers for steady-state computations. The third-order minmod differencing option in the code was used for all calculations with a Courant number of 5. Euler solutions were obtained at Mach numbers from 1.80 to 4.20 and angles of attack up to 10 degrees. All cases were run to convergence at 1,000 iterations with a speed of approximately 1.9 x 10-5 sec per iteration.

Multi-Body Pressure Comparisons

To illustrate the aerodynamic interference in the multi-body cases, Figure 9 plots the pressure coefficients on the inboard side of the upper body for the three finned configurations at Mach 3.50 and zero degrees angle of attack. It is clear that by adding a second body and then a third, the flow is forced to accelerate between the bodies as

data shows no change in the shock location as additional bodies are added, although the magnitude of the expansion increases. With this body location being the farthest from the third body, the relatively small increase in flow expansion is not surprising.

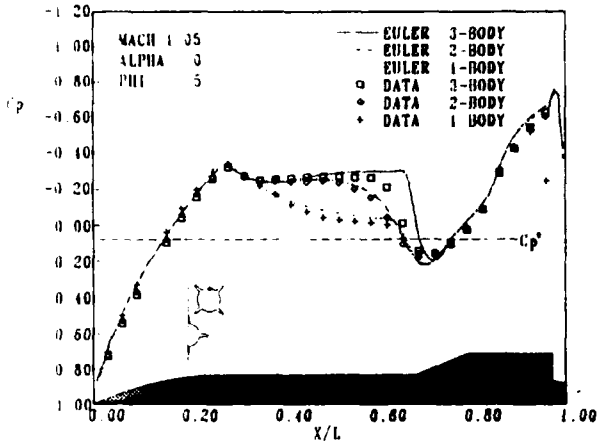

Fig. 12 Configuration Effects, Upper Body, Upper Side

When the three-body case was placed at angle of attack, the agreement with data was, in general, as good as before. Figure 13 shows the structure of the pressure distribution on the top side of the upper body at Mach 0.95. In addition, pressure distributions for the single body case are also plotted for freestream reference. In both the one and three body cases, the curves are consistent as angle of attack increases to ten degrees. At angle of attack, both cases show increased expansion and forward movement of the shocks when compared to zero angle of attack curves. On the windward side of the upper body, Figure 14, the flow expansions decreased and the body shock moved rearward with increasing angle of attack. In the single body case the wind tunnel data confirms this prediction, but in the three-body case it does not. The data shows the opposite effect with the shock moving slightly forward, influenced by the interference flowfield. Clearly, the inviscid code has difficulty predicting the shock location in the viscous region between the bodies.

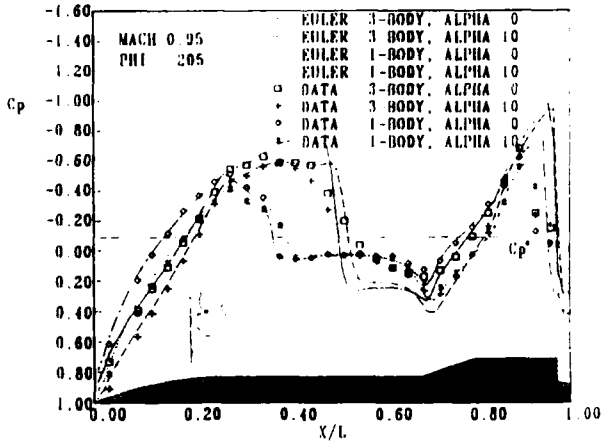

Fig. 14 Angle of Attack Effects, Upper Body, Lower Side

On the bottom body, however, an unexpected pattern was observed, Figure 15. As the angle of attack increased, the magnitude of the body pressure expansion on the leeward side actually decreased, opposite to that observed in the single body case and on the upper body, Figure 12. In addition, the shock moved aft rather than forward, although the data shows little, if any, movement. It appears that the upper bodies in the three-body case appear to dominate the overall flowfield in this case by not only establishing the strong body shock in the interferenced region that falls farther downstream on the lower body, but also inhibiting the normal expansion that would occur on a body leeside at angle of attack. This is probably due to a channeling effect between the three bodies that in essence not only reduces the effective angle of attack on the lower body, but also limits the leeside expansion on the lower body to the magnitude of the windward expansion on the upper body.

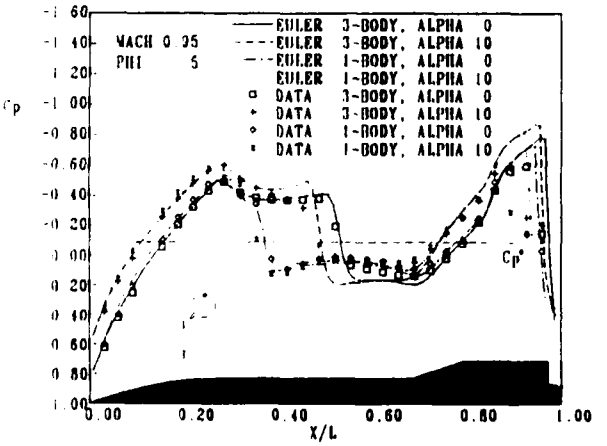

Fig. 13 Angle of Attack Effects, Upper Body, Upper Side

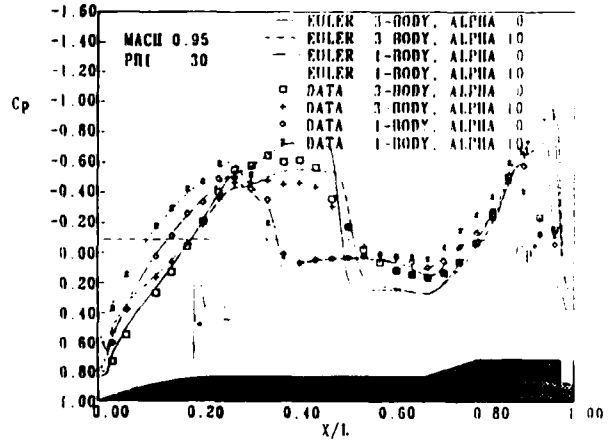

Fig. 15 Angle of Attack Effects, Lower Body, Upper Side

Mach 0.80. The two expansion regions on the inboard side at the nose and tail provide a strong inboard force when compared to the same two outboard locations. This identical pattern was also observed on the upper/lower sides of both the upper and lower bodies, where the expansion peaks on the maximum interference sides determined the force direction. The result was an inward/downward force on the upper body and upward force on the lower body. Supersonically, the forces reverse themselves. The pressure distribution on inboard and outboard sides of the upper body, Figure 21, give evidence for this reversal. In marked contrast to Mach 0.80, the flow expansion in the fin region is nearly the same from one side of the body to the other. In addition, the pressure on the outboard side of the nose expands more rapidly than the inboard side, resulting in a net outboard force. However, the significant

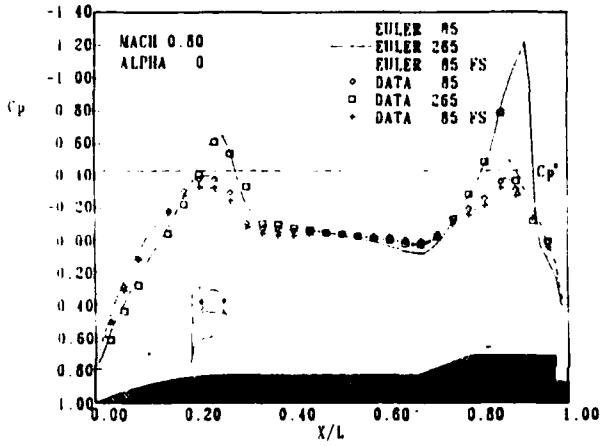

Fig. 20 Subsonic Interference Effects, Upper Body

contributions to the outward force occurs as a result of the shock on the body near the fin leading edge region. Unlike at Mach 0.80 where little difference was observed across the body in the compression region after the body shock, a significant difference occurs here across the body, resulting in an outward force. Only the large expansion region prior to the shock on the inboard side, X/L = 0.30 to 0.60, serves to minimize the outward force. Again the identical behavior was seen on the upper/lower sides of the upper and lower bodies. Figure 22 supports this observation on the lower body and shows the good agreement between prediction and data that was consistent throughout the investigation. The result is that at Mach 1.20, the resultant force is outward/upward on the upper body, and downward on the lower body.

Investigation of the moment coefficients yielded an equally interesting explanation. Figure 19 shows that the bodies react to the subsonic flow opposite to that in supersonic flow. Subsonically, the nose of each body moves away from the other, while the fin sections move toward each other. In supersonic flow the direct opposite occurs, where the body nose sections come together while the fin sections move apart. At Mach 0.80, Figure 20, the flow expansion on the

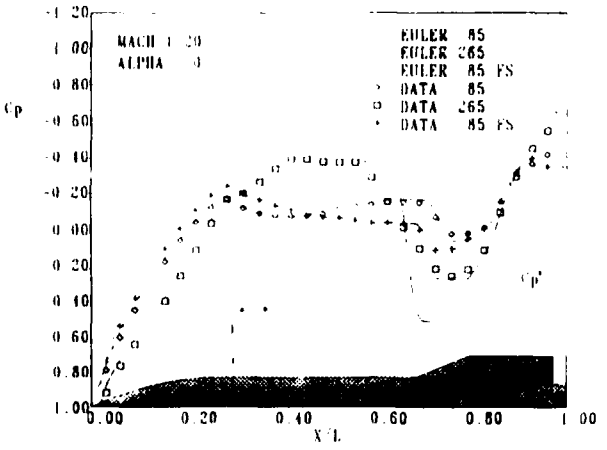

Fig. 21 Supersonic Interference Effects, Upper Body

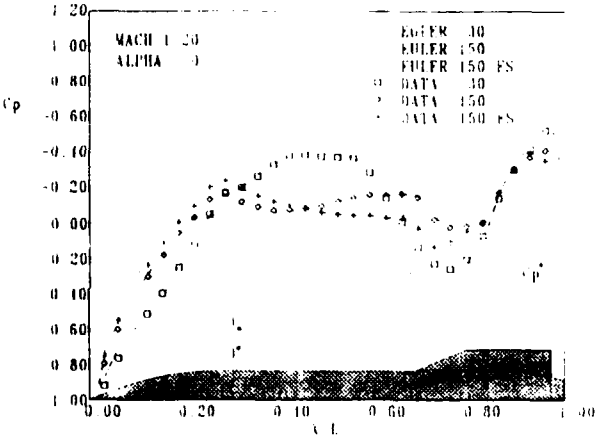

Fig. 22 Supersonic Interference Effects, Lower Body

inboard side of the upper body dominates the pitching and yawing moments. The difference across this fin section from outboard to inboard is so great that the fin sections move toward each other. Since this also occurs in the vertical plane of both the upper and lower bodies, the result is that the nose of the upper body pitches upward and yaws outboard, while the nose of the lower body pitches downward. This phenomena has been observed on numerous occasions in subsonic flight of actual aircraft with multiple bodies in carriage. Reversal of this trend supersonically can be explained from Figures 21 and 22. The dominant feature here is the strong shock on the body at X/L = 0.67, with the accompanying expansion area before and sharp compression region after. This expansion/compression forms a couple that rotates the nose inward and the fin section outward. The magnitude of the moment is restricted by the proximity of the forces to the moment reference center, and the counteracting nose compression on the inboard side. Since the vertical plane of both the upper and lower bodies are similarly effected, the result is that the

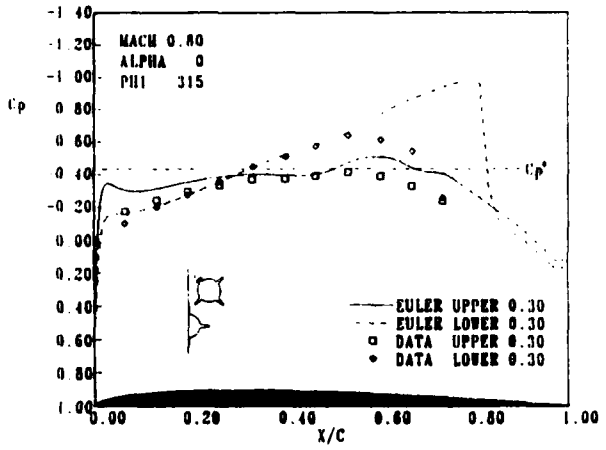

Fig. 27 Fin Subsonic Interference Effects

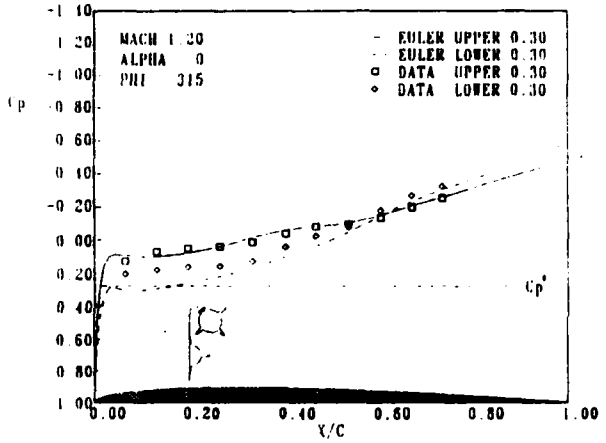

Fig. 28 Fin Supersonic Interference Effects

Conclusions

Interference flow predictions were successfully made on multiple body configurations in the transonic regime, where the strongest interference effects were found to exist near Mach 1. Agreement with data was very good in the minimum interference regions located on the outboard sides of the bodies. In the maximum interference regions between the bodies, the agreement with data was good in general, but shock location and structure were strongly influenced by viscous effects in the three-body case. It was found that the interference effects were not localized to the inboard sides of the bodies, but strongly influenced the expansion region and subsequent shock on the outboard sides. Consequently, the outboard sides of the bodies were not in a freestream condition. The addition of fins served only to increase the blockage in the flow; moving the body shock forward, but with no change in flow expansion.

At angles of attack, it was found that the interference effects on the lower body were quite the opposite to what was expected. In the three-body case, the flow was channeled between the bodies. As a result, the expansion on the upper or leeside of the lower body actually diminished with angle of attack, limited to the expansion on the windward side of the upper body.

It was also found that the rigid-body physics of the three-body configuration was dependent on Mach number. This was primarily caused by the rearward movement of the expansion regions and subsequent shocks as the Mach increased from 0.80 to 1.20. Subsonically, the bodies tended to be pulled together at the fin sections, resulting in nose-outward moments. Supersonically, the bodies repulsed each other with resulting nose-inward moments. These physical reactions to the interference flowfield, as well as the flowfield itself, were found to be adequately predicted by the Euler code. The dominant trends were predicted, although the fine details in the viscous regions were not.

References

1. Thompson, J. F., "A Composite Grid Generation Code for General Three-Dimensional Regions - the EAGLE Code," AIAA Journal, Volume 26, No. 3, p. 271, March 1988.

2. Thompson, J. F., and Gatlin, B., "Program EAGLE User's Manual, Volumes II and III, Surface and Grid Generation Codes," AFATL-TR-88-117, September 1988.

3. Belk, D. M., and Whitfield, D. L., "Three-Dimensional Euler Solutions on Blocked Grids Using an Implicit, Two-Pass Algorithm," AIAA-87-0452, January 1987.

4. Mounts, J. S., Belk, D. M., and Whitfield, D. L., "Program EAGLE User's Manual, Volume IV, Multi-Block, Implicit, Steady-State Euler Code," AFATL-TR-88-117, September 1988.

5. Lijewski, L. E., "Transonic Flow Solutions on a Blunt, Finned Body of Revolution Using the Euler Equations," AIAA-86-1082, May 1986.

6. Lijewski, L. E., "Transonic Flow Solutions on a Blunt, Body-Wing-Canard Configuration Using the Euler Equations," AIAA-87-2279, August 1987.

7. Cottrell, C. J., Martinez, A., and Chapman, J. T., "A Study of Multi-Body Aerodynamic Interference at Transonic Mach Numbers," AIAA-87-0519, January 1987.

8. Benek, J. A., Donegan, T. L., and Suhs, N. E., "Extended Chimera Grid Embedding Scheme with Application to Viscous Flows," AIAA-87-1126, June 1987.

9. Cottrell, C. J., and Lijewski, L. E., "Finned, Multi-Body Aerodynamic Interference at Transonic Mach Numbers," Journal of Aircraft, Volume 25, No. 9, pp. 827-834, September 1988.